

# Lightweight Joint Optimization of General-Purpose Vision-Language Models and Retrievers for Medical Diagnosis

Nir Mazor<sup>1</sup>, Tom Hope<sup>1,2</sup>

<sup>1</sup>School of Computer Science and Engineering, The Hebrew University of Jerusalem

<sup>2</sup>The Allen Institute for AI (AI2)

nir.mazor@mail.huji.ac.il, tomh@allenai.org

## Abstract

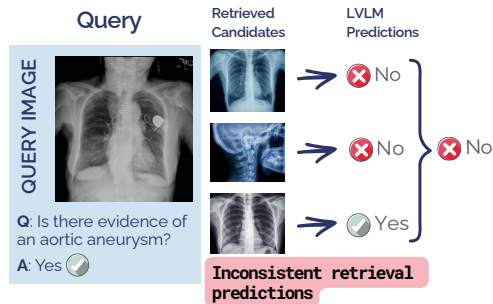
Clinical decision-making often involves interpreting images (e.g., radiology) for making diagnoses. Retrieving relevant visual information from medical literature and hospital records could enhance diagnostic accuracy. In this paper, we develop a model in which a multimodal retriever is jointly optimized with an LVLM for medical diagnosis, unlike standard RAG where LVLM error signal is not propagated down to the retriever. We show that using only general-purpose backbones, with only lightweight fine-tuning, our model is able to achieve competitive results with medically-pretrained models across clinical multi-label classification and visual question answering tasks. In a novel analysis, we additionally find that in many cases different top retrieved images each lead to different predictions for a given target, and that these cases are empirically challenging for all models, even for non-retrieval models. Our joint retrieval optimization significantly improves these challenging cases over standard RAG. However, oracle analysis reveals that while the correct diagnosis is frequently achievable using one of the top retrieved images, in practice there is a large performance gap from the oracle, and rerankers using frontier LVLMs do not close this gap—leaving ample room for improvement by future methods. Code will be made publicly available.

## Introduction

Inferring diagnoses from medical imagery is a fundamental part of clinical decision-making. Large Vision Language Models (LVLMs) have been widely explored for medical diagnosis (Thawakar et al. 2024; Wu et al. 2023; Zhang et al. 2023b; Moor et al. 2023; Li et al. 2023). To improve the performance of LVLMs in the medical field, retrieval augmentation has been adopted and has shown promising results, providing more accurate and also explainable methods (He et al. 2024a; Xia et al. 2024b,a; Wu et al. 2025).

In this work, we explore a lightweight fine-tuning approach for taking a *general*-purpose LVLM and optimizing it *jointly* with a *general*-purpose multimodal retriever. Different from the common retrieval augmented generation (RAG) setup, we perform *joint optimization* of the LVLM and retriever. This joint optimization teaches the LVLM to utilize retrieved knowledge for making accurate medical predictions while at the same time tuning the multimodal retriever to retrieve information that leads to correct predictions by the LVLM. The retriever model retrieves images

## Fine-Tuned Multimodal RAG



## JOMED: Joint Optimization

LVLM and multimodal retriever jointly optimized for downstream tasks

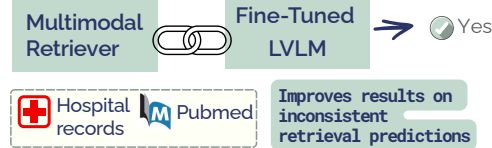


Figure 1: We jointly optimize a multimodal retriever and a Large Vision-Language Model (LVLM) for medical tasks. Our model achieves competitive results without resource-intensive medical pre-training and significantly improves performance on challenging cases where different retrieved images lead to inconsistent retrieval prediction.

as well as captions and clinical reports from both literature and hospital records. Our method involves sequential multimodal training with a dual-head retriever architecture and a retrieval loss that enhances the retriever’s ability to provide more predictive context to the LVLM.

Poorly optimized retrieval mechanisms can mislead models (Yoran et al. 2023; Sun et al. 2024). Figure 2 demonstrates this problem with an ultrasound image that shows no breast cancer. When the retrieval system selects an irrelevant reference image showing cancer features, the model incorrectly identifies cancer in the input image. When we jointly optimize the retriever to find more relevant images and text, the model’s prediction flips to the correct diagnosis.

Using our approach, we are able to achieve competitive results in medical image classification and visual question answering (VQA). Importantly, our focus in this work is not to chase SOTA results but to shed light on several interesting observations. One, that a simple and effective joint LVLM-retriever optimization mechanism can lead to a substantial boost in results over standard multimodal RAG and should thus be more widely adopted for medical diagnosis.

Second, that this mechanism achieves competitive results by using models with no medical pre-training (for neither the LVLM nor the retriever) and only lightweight fine-tuning; this resonates with recent findings showing general-purpose LVLMs can rival their medical counterparts (Jeong et al. 2024) and has potentially important implications considering the resource-intensive nature of pre-training processes.

Third, previous work on joint training in the general domain required large-scale pre-training followed by few-shot task-specific adaptation (Izacard et al. 2023; Hu et al. 2023; Lin et al. 2024). In contrast, our novelty is in conducting joint training *directly on downstream tasks* with no pre-training and only lightweight fine-tuning (as few as 546 samples). This provides first evidence about the feasibility and utility of lightweight data-efficient joint training directly on downstream tasks as opposed to in the pre-training setting. We are also the first to explore and show the utility of joint training in the multimodal medical domain.

Fourth and importantly, we conduct a novel analysis that finds that our method helps in particular to address a class of errors we term *inconsistent retrieval predictions*. Inconsistent retrieval predictions are cases in which for a given patient image, each retrieved image leads the model to make different predictions. These cases commonly occur across our experiments and are substantially more difficult for models, both retrieval-augmented and non-retrieval models. This instability with respect to different retrieval candidates leads to high prediction entropy/uncertainty across classes, degrading not only overall RAG results but also their reliability (Lambert et al. 2022).

As we show, our joint training mechanism significantly mitigates this issue and achieves large improvement over standard fine-tuned RAG on these cases.

We further discover that for a large proportion of these inconsistent cases, at least one retrieved candidate enables the model to predict the correct answer in an oracle setting in which we provide the model with the correct retrieved candidate. This suggests useful information is being retrieved but is often lost among less helpful candidates. To address this, we explored using the powerful multimodal model o3 (OpenAI 2025) as a reranker to identify the most predictive instances. We found it did not close the performance gap to the oracle and was comparable or inferior to our method, leaving significant room for future improvement.

#### Our contributions

- We develop a method where a multimodal retriever and a Large Vision-Language Model (LVLM) are jointly optimized for medical classification and VQA. Unlike standard Retrieval-Augmented Generation (RAG), our method propagates error signal from the LVLM down to the retriever while training on downstream tasks.

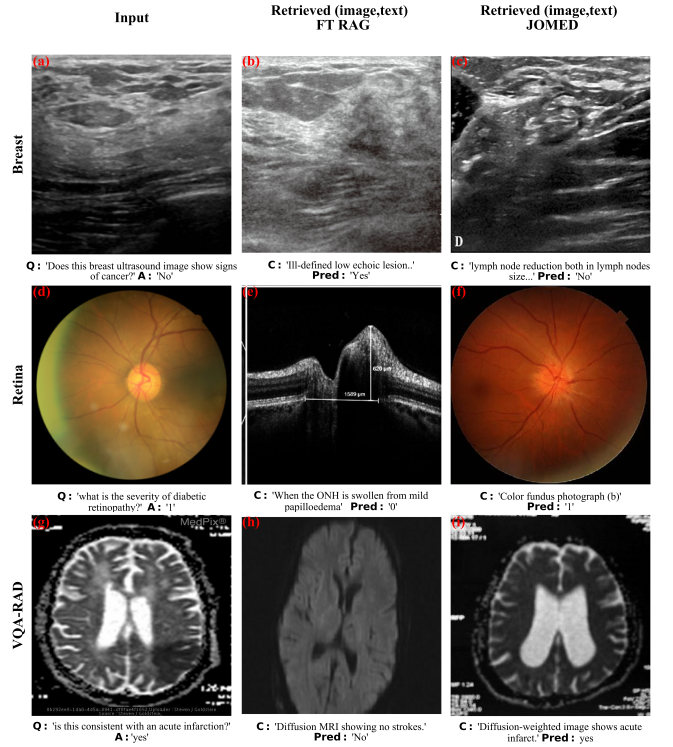


Figure 2: Joint training impacts inconsistent retrieval predictions. After joint training, retrieved images show greater alignment with query image labels. In Breast, a cancer-free ultrasound query (a) initially retrieved a lesion image (b), however, after joint training, the retrieved image is less directly related to the wrong label (c). For Retina, joint training changed retrieval from a different modality (e) to be more similar to the query (d). In VQA-RAD, retrieval shifted from an unrelated medical condition (h) to an image depicting the condition of the query image.

- We show that our method achieves competitive results compared to medically pre-trained models by using only general-purpose backbones. Unlike previous general-domain joint training methods that require pre-training, we conduct joint training directly on downstream tasks with only lightweight data-efficient fine-tuning.
- In a novel analysis we identify *inconsistent retrieval predictions*, challenging cases where different retrieved images lead to different predictions for the same query. Our joint optimization method significantly improves performance on these cases when compared to standard RAG.

## Related Work

**Retrieval Augmented Joint Training** has been explored primarily in unimodal (text only) NLP with work such as ATLAS (Izacard et al. 2023), which conducted large-scale pretraining of both reader and retriever models and evaluated in zero-shot and few-shot scenarios in the general domain. REVEAL (Hu et al. 2023) extended this to the multimodal setting, achieving state-of-the-art results in visual tasks in

the general domain with extensive pre-training. (Shi et al. 2023) proposed training textual retrievers based on reader performance, influencing subsequent joint-training methods (Lin et al. 2024). introduced another joint training variant and proposed sequential training: first training the reader with retrieval augmentation, then training the retriever. Siriwardhana et al. (2023) demonstrated joint training’s effectiveness for domain adaptation. Our work differs by being the first to explore joint training optimized directly for downstream tasks, with minimal fine-tuning, as opposed to requiring large-scale pre-training. Our extensive novel analyses are the first to shed light on inconsistent predictions and how joint training on downstream tasks helps address them.

**Multimodal Retrieval Augmentation in Medical Applications.** Multimodal retrieval augmentation began with encoder-based architectures (Yuan et al. 2023), which integrated retrieved text and images with query modalities. With Large Vision-Language Models (LVLMs), (He et al. 2024a) proposed retrieving relevant labeled examples during inference. (Xia et al. 2024b) addressed LVLMs’ misalignment with medical knowledge using retrieval-augmented generation to fetch similar medical reports, employing contrastive learning and context selection strategies. (Xia et al. 2024a) proposed domain-aware retrieval for diverse medical data sources, while (Wu et al. 2025) combined retrieval augmentation with knowledge graphs to reduce hallucination.

## Method

**Overview.** In this section, we present our methodology, named JOMED (Joint Optimization of Multimodal Retrieval for Enhanced Medical Diagnosis). Our task involves classifying medical images and medical visual question answering. JOMED consists of two main components: a multimodal retriever and a reader. We are given an input patient image and a diagnostic question. The multimodal retriever is tasked with identifying relevant medical knowledge from either literature or hospital records—in the form of images and associated captions or hospital reports that provide predictive information. The reader then analyzes the retrieved candidates along with the diagnostic question and generates an answer. We jointly optimize the reader to better utilize retrieved candidates, and the multimodal retriever to improve its ability to retrieve informative candidates for the reader. Figure 3 illustrates our method. The multimodal retriever has two retrievers, textual and visual, for finding candidates in an index of image-caption pairs derived from literature and hospital records. Given an image query, these retrievers find candidates that are then passed to the reader.

Unlike previous work (He et al. 2024a; Xia et al. 2024b,a) our method does not use medical pretraining, and instead we use readily available general LVLMs (Pixtral and Qwen2-vl) and a general retriever, jina-clip (Xiao, Mastrapas, and Wang 2024). The selected LVLMs can process multiple images and texts, allowing us to incorporate both the retrieved image and the retrieved caption/report into the model context. We also compare our results to Med-Flamingo (Moor et al. 2023). MedFlamingo is a medical LVLM which is also able to process multiple images, unlike other medical LVLM available at the time of conducting our experiments.

Finally, we also explore the utility of o3 (OpenAI 2025) as a reranker. We now elaborate on the details.

## Reader Retrieval Augmentation Fine-Tuning

We first fine-tune the reader with retrieval augmentation. This step aims to achieve two main goals: improving the reader’s performance on the dataset and teaching the reader to effectively utilize retrieved (image, text) pairs in context.

For an image, question tuple  $(i_d, q_d)$   $d \in \{1, \dots, D\}$  from dataset  $D$ , we retrieve  $K$  relevant tuples of images and texts (reports or captions)  $(i_k, t_k)$   $k \in \{1, \dots, K\}$  using our multimodal retriever module. These retrieved pairs are prepended to the image-question pair  $(i_d, q_d)$  to create augmented inputs. The augmented input consists of the retrieved context followed by the target question-image pair:  $(i_k, t_k), (i_d, q_d)$   $k \in \{1, \dots, K\}$ . To the best of our knowledge, we are the first to use both the retrieved image and caption/report in context within medical RAG for LVLMs. We use supervised fine-tuning on the augmented input, minimizing the negative log-likelihood to predict the answer  $a_d$ :

$$\mathcal{L}(\theta) = - \sum_{d=1}^D \sum_{k=1}^K \log p_\theta(a_d | (i_k, t_k) \circ (i_d, q_d))$$

where  $\theta$  represents the parameters of the LVLM, and  $\circ$  denotes the concatenation operation in the context window.

## Sequential Multimodal Retriever Fine-Tuning

Our dual-head multimodal retriever has a text-based head for retrieving relevant (image, text) pairs based on textual similarity to the query, and an image-based head for retrieving pairs based on visual similarity. To train this multimodal retriever, we measure how each retrieved (image, text) pair contributes to the LVLM’s performance, optimizing the retriever to prioritize high-contribution candidates.

We adopt a sequential training strategy, first optimizing the text retrieval head followed by the image retrieval head. During this process, the reader model remains frozen, focusing solely on improving the retriever’s embedding space. We formulate a Sharp Perplexity Loss as a simple variant of the perplexity distillation loss (Izacard et al. 2023). Similarly to Izacard et al. (2023) we minimize the KL-divergence between the LVLM’s posterior distribution over retrieved pairs and the retriever’s distribution, however we do so directly on downstream tasks with only lightweight fine-tuning in the data-efficient regime without pre-training.

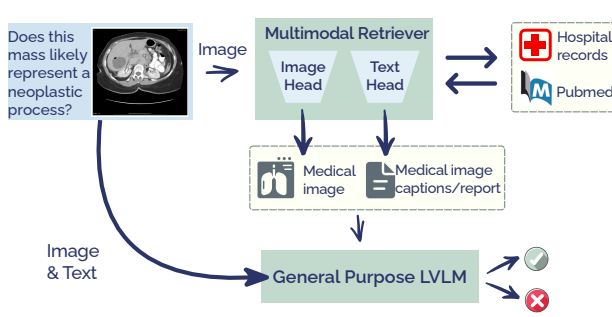
The posterior distribution reflects the model’s confidence in predicting the correct answer  $a$  given a retrieved (image, text) pair  $(i_k, t_k)$  and a query image-question pair  $(i, q)$ :

$$p_k \propto p_{\text{LVLM}}(a | (i_k, t_k) \circ (i, q)),$$

where  $p_{\text{LVLM}}(a | (i_k, t_k) \circ (i, q))$  is the probability assigned by the LVLM to  $a$ , and  $\circ$  denotes prepending the retrieved chunk to the query.

We sharpen the LVLM’s output distribution by restricting it to only the relevant class tokens from the benchmark’s possible answers. Specifically, we extract the model’s logits, select only the relevant tokens for each class, and apply

## ① Reader Retrieval Augmentation Fine-Tuning



## ② Sequential Multimodal Retriever Fine-Tuning

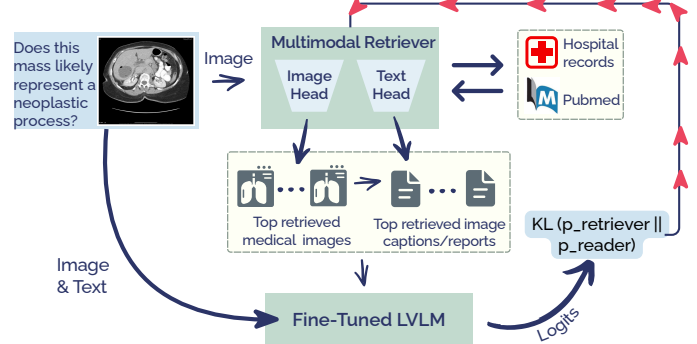


Figure 3: JOMED combines a general-purpose VLLM with a general-purpose multi-modal retriever in a two-phase approach. First, with a frozen retriever, we augment training by prepending retrieved (image, caption/report) pairs to original queries, training the LVLM on these augmented prompts. Second, with the LVLM frozen, we sequentially train the dual-head multi-modal retriever using Sharp Perplexity Distillation loss (KL-divergence between the distribution derived from the model logits and the distribution derived from the retrieved candidates’ similarity).

a softmax to obtain a more discriminative distribution (for VQA tasks, we use yes/no tokens and skip open questions.). We denote this class-restricted distribution as  $p_{LVLM_C}$  where  $C = \{c_1, c_2, c_3, \dots\}$  is the set of chosen class tokens. The normalized posterior  $p_k$  is formulated as:

$$p_k = \frac{\exp(\log p_{LVLM_C}(\mathbf{a} | (\mathbf{i}_k, \mathbf{t}_k) \circ (\mathbf{i}, \mathbf{q})))}{\sum_{i=1}^K \exp(\log p_{LVLM_C}(\mathbf{a} | (\mathbf{i}_i, \mathbf{t}_i) \circ (\mathbf{i}, \mathbf{q})))},$$

where  $K$  is the total number of retrieved pairs.

The retriever’s distribution is defined by:

$$p_{RETR}((\mathbf{i}, \mathbf{t}) | (\mathbf{i}, \mathbf{q})) = \frac{\exp(s((\mathbf{i}, \mathbf{t}), (\mathbf{i}, \mathbf{q})) / \tau)}{\sum_{k=1}^K \exp(s((\mathbf{i}_k, \mathbf{t}_k), (\mathbf{i}, \mathbf{q})) / \tau)},$$

where  $s((\mathbf{i}, \mathbf{t}), (\mathbf{i}, \mathbf{q}))$  is the similarity score between the pair and the query, and temperature  $\tau$  controls distribution sharpness. For the text retrieval head, the score is computed using the dot product between the index caption/report embeddings and the query image embedding, while for the image retrieval head, we use the index image embeddings.

Finally, for our loss we compute the KL-divergence between retriever and reader distributions  $KL(p_{LVLM_C} || p_{RETR})$ :

$$\sum_{k=1}^K p_{LVLM_C}((\mathbf{i}_k, \mathbf{t}_k)) \log \left( \frac{p_{LVLM_C}((\mathbf{i}_k, \mathbf{t}_k))}{p_{RETR}((\mathbf{i}_k, \mathbf{t}_k))} \right)$$

## Inference

Following Shi et al. (2023) for a given (image, question) pair, we retrieve the top- $k$  relevant (image, text) chunks using the image as the query. Each chunk is prepended to the question, and the LVLM computes predictions for the augmented prompts in parallel. The final output probability is:

$$p_{LVLM}(a | \mathbf{q}) = \sum_{k=1}^K p_{LVLM}(a | (\mathbf{i}_k, \mathbf{t}_k) \circ \mathbf{q}) \cdot p_R((\mathbf{i}_k, \mathbf{t}_k) | \mathbf{q}),$$

where  $p_R((\mathbf{i}_k, \mathbf{t}_k) | \mathbf{q})$  is:

$$p_R((\mathbf{i}_k, \mathbf{t}_k) | \mathbf{q}) = \frac{\exp(s(\mathbf{q}, (\mathbf{i}_k, \mathbf{t}_k)))}{\sum_{j=1}^K \exp(s(\mathbf{q}, (\mathbf{i}_j, \mathbf{t}_j)))},$$

and  $s(\mathbf{q}, (\mathbf{i}_k, \mathbf{t}_k))$  is the similarity score between the query and the retrieved chunk.

## Experiments

### Experimental Setup

Our datasets include real-world hospital datasets (BRSET (Nakayama et al. 2024) and VinDr-PCXR (Pham, Tran, and Nguyen 2022)) alongside a variety of classification and visual question answering datasets. We focus on a low-resource data-efficient setting (training sets ranging from 546 to 7007 samples in classification, 1790-19,700 in VQA). Medical image annotation is a resource-intensive task, demanding expert annotators whose availability is limited and expensive. Clinical AI also often has poor generalization across heterogeneous medical centers and patient populations, often requiring that models be trained for the specific context in which they are deployed (Casey 2022). Such constraints often restrict researchers to datasets comprising only a few thousand samples for a given study. Retrieval augmentation is well-suited for this setting, as it is known to benefit low-data regimes the most by leveraging external knowledge to compensate for sparse training samples.

We consider three types of classification tasks: binary, multi-class, and multi-label. These include BreastMNIST (nickname: Breast; breast ultrasound imaging, binary) (Al-Dhabayani et al. 2020), DermaMNIST (nickname: Derma; pigmented skin lesion images, multi-class)

(a)												
Backbone	Model	Breast		Derma		Retina		VinDr-PCXR		BRSET		Mean
		ACC	F1									
Qwen2-vl	Reader	.83	.77	.68	.27	.60	.44	.48	.08	.34	.23	.59 .36
	FT RAG	.85	.82	.71	.42	.62	.48	.55	.09	.48	.27	.64 .42
	JOMED	<b>.87</b>	<b>.84</b>	<b>.76</b>	<b>.50</b>	<b>.65</b>	<b>.50</b>	<b>.57</b>	<b>.14</b>	<b>.49</b>	<b>.37</b>	<b>.67 .47</b>
	JOMED <sub>oracle</sub>	.87	.84	.85	.64	.69	.51	.64	.14	.52	.41	.71 .51
Pixtral	Reader	.82	.77	.75	.52	.55	.44	.48	.08	.44	.33	.61 .43
	FT RAG	.88	.85	.79	.60	.57	.47	.49	.09	.47	.33	.64 .47
	JOMED	<b>.90</b>	<b>.87</b>	<b>.80</b>	<b>.62</b>	<b>.60</b>	<b>.51</b>	<b>.56</b>	<b>.14</b>	<b>.51</b>	<b>.37</b>	<b>.67 .50</b>
	JOMED <sub>oracle</sub>	.93	.90	.83	.67	.63	.54	.67	.15	.57	.41	.73 .53

(b)											
Backbone	Model	VQA-RAD		SLAKE		PathVQA		Mean		Closed	Open
		Closed	Open	Closed	Open	Closed	Open	Closed	Open		
Qwen2-vl	Reader	.73	.41	.84	.80	.87	.25	.81	.49		
	FT RAG	.76	.45	.88	.81	.91	.33	.85	.53		
	JOMED	<b>.78</b>	<b>.47</b>	<b>.90</b>	<b>.83</b>	<b>.93</b>	<b>.37</b>	<b>.87</b>	<b>.56</b>		
	JOMED <sub>oracle</sub>	.86	-	.92	-	.95	-	.91	-		
Pixtral	Reader	.72	.38	.83	.80	.87	.26	.81	.48		
	FT RAG	.74	.41	.88	.81	.88	.31	.83	.51		
	JOMED	<b>.76</b>	<b>.43</b>	<b>.90</b>	<b>.82</b>	<b>.90</b>	<b>.35</b>	<b>.85</b>	<b>.53</b>		
	JOMED <sub>oracle</sub>	.88	-	.92	-	.95	-	.92	-		

Table 1: Results for classification (a) and visual question answering (b). Joint training consistently leads to the best results, with up to a 10-point increase in F1 score compared to fine-tuned (FT) RAG for multi-label classification. For visual question answering, we evaluate closed questions using the exact match metric and open questions using token recall. Using an oracle reranker demonstrates that even larger improvements are achievable with JOMED’s top-retrieved images in some datasets. Note that in the open question scenario, we do not evaluate the oracle because there is no clear discriminative boundary between different answers to determine the correct one, as there is in classification and closed question answering tasks. Using an oracle reranker shows that larger improvement is achievable with JOMED’s top retrieved images in some datasets.

Medical Pretrained Size	Model	Breast	Derma
177K	MedVInT-TE	.88	.78
177K	MedVInT-TD	.90	.80
177K	MedDr <sub>InternVL</sub>	.72	-
177K	MedDr + RAD <sub>InternVL</sub>	.88	-
255K	GSCo <sub>InternVL</sub>	.93	-
0	JOMED Qwen2-vl	.87	.76
0	JOMED <sub>Pixtral</sub>	.90	.80

Table 2: Accuracy of JOMED and prior reported results of medical pre-trained models for multiclass classification.

(Tschandl, Rosendahl, and Kittler 2018), RetinaMNIST (nickname: Retina; retinal fundus images with multi-label disease annotations) (Liu et al. 2022), and two challenging real-world multi-label datasets: VinDr-PCXR (a chest X-ray dataset with 15 labels) (Pham, Tran, and Nguyen

Medical Pretrained Size	Model	VinDr-PCXR	BRSET
255K	MedDr <sub>InternVL</sub>	.08	.08
255K	GSCo <sub>InternVL</sub>	.09	.33
0	JOMED Qwen2-vl	.14	.37
0	JOMED <sub>Pixtral</sub>	.14	.37

Table 3: F1 Comparison of JOMED to prior reported results of medical pre-trained models for multi-label classification.

2022) and BRSET (an ophthalmology dataset with 14 labels) (Nakayama et al. 2024). For visual question answering, we use widely adopted benchmarks: VQA-RAD (Lau et al. 2018), SLAKE-English (Liu et al. 2021), and PathVQA (He et al. 2020). Full details are provided in Appendix .

Retrieval augmentation is supported by an external index constructed from PubMed and medical records: PMC-OA (Lin et al. 2023), MIMIC-CXR (Johnson et al. 2019), and ROCO (Rückert et al. 2024). Full descriptions are available

Medical Pretrained Size	Model	SLAKE		PathVQA	
		Closed	Open	Closed	Open
			.90	.85	.88
600K	BiomedGPT-B	.90	.85	.88	.28
600K	LLaVA-Med <sub>LLaVA</sub>	.83	.85	.91	.38
600K	LLaVA-Med <sub>Vicuna</sub>	.85	.83	.92	.39
600K	LLaVA-Med <sub>BioMedCLIP</sub>	.87	.87	.91	.39
0	JOMED <sub>Qwen2-vl</sub>	.90	.83 (.84)	.93	.37 (.37)
0	JOMED <sub>Pixtral</sub>	.90	.82 (.82)	.90	.35 (.35)

Table 4: Comparison of JOMED to medical pre-trained models for visual question answering. We report the token recall metric, reported for LLaVA-Med variants and token F1 reported for BiomedGPT (in red).

in Appendix . Our experiments leverage two backbone models—Pixtral (12B) (Agrawal et al. 2024) and Qwen2-vl (7B parameters) (Wang et al. 2024) with jina-clip-v1 (Xiao, Mastrapas, and Wang 2024) serving as the general-purpose retriever’s visual head, embedding both the texts and images of the retrieval index. All models were trained in a low-resource setting, with all runs performed on a single L40s GPU. More details in Appendix .

For comparison to medically pre-trained LVLMs, we include competitive baseline models: BiomedGPT (Luo et al. 2023); three LLaVA-Med (Li et al. 2023) variants; two LVLM variants based on PMC CLIP (MedVInT-TE and MedVInT-TD) (Zhang et al. 2023b); and three variants based on InternVL (Chen et al. 2024): MedDr, MedDr + RAD (He et al. 2024a), and GSCo (He et al. 2024b). Full details are in Appendix .

## Results

Table 1a and Table 1b demonstrate the effectiveness of JOMED for two backbone models, Pixtral and Qwen2-vl, across five medical imaging classification benchmarks and three visual question answering benchmarks. JOMED achieved superior results compared to both the standard fine-tuned multimodal RAG baseline (trained only with retrieval augmentation fine-tuning, as detailed in Section ) and the Reader baseline (LVLM trained without retrieval), for both backbones and all benchmarks.

In Table 1a, for classification tasks, JOMED with the Qwen2-vl backbone achieved a mean improvement of 0.05 in F1 and 0.03 in ACC over fine-tuned multimodal RAG, with F1 gains of 0.10 and 0.08 in two datasets. JOMED with Pixtral achieved a mean improvement of 0.03 in F1 and ACC. In Table 1b, for VQA tasks, JOMED with Pixtral and Qwen2-vl achieved a mean improvement of 0.02 in ACC (Exact Match) for closed question answering. For open question answering, JOMED with Qwen2-vl achieved a mean improvement of 0.03 in token recall, while JOMED with Pixtral achieved an improvement of 0.02.

In addition, we evaluated our model in an oracle scenario.

Instead of the final fusion of logits (Section ), we applied an oracle that, given the model responses for different retrieved images, selects the correct answer if it exists. Our findings in Tables 1a and 1b show that the correct answer exists in a large proportion of cases, yielding superior results. This shows that in these cases, JOMED is able to surface in its top retrieved images an image which could lead to a correct prediction, however the information gets lost in the process of prediction fusion with other retrieved images. Simply taking the label with highest confidence or label with highest average confidence across retrieved images, underperforms. This motivates us to explore the use of the o3 multimodal reasoning model to detect this image (see below).

**Benchmarking versus pretrained LVLMs for classification.** In Tables 2 and 3, we include previously reported results for several leading medically pretrained LVLM methods (detailed in Section ). JOMED with both backbones delivered competitive performance relative to models that underwent extensive pretraining. For multi-label classification, JOMED outperformed the pre-trained models. For binary and multi-class classification tasks, JOMED with Pixtral matched or exceeded all models except GSCo, which achieved 0.03 higher ACC on the Breast dataset. Overall, our models performed strongly across four medical benchmarks compared to medical pretrained models. We are not aware of any medical LVLM evaluated on Retina. To our knowledge, no other LVLMs have been evaluated on our benchmarks. Additionally, in Table 2 we report only ACC, as F1 scores were not reported for the compared models. Similarly, in Table 3, we report only F1 scores. We also evaluated a medical baseline, Med-Flamingo, with a pretrained medical retriever (BiomedCLIP (Johnson, Douze, and Jégou 2019)). We observed that Med-Flamingo generally underperformed, and showed limited improvement from utilizing the retrieved context to enhance performance, which we suspect may be attributed to its relatively older LLaMA backbone (Touvron et al. 2023). We further try BiomedCLIP as a retriever with our general-purpose LVLMs, which showed improvements over FT RAG, with a similar pattern to the general-purpose retriever. Full results in Appendix .

**Benchmarking versus pretrained LVLMs for visual question answering.** In Table 4, we also compare our approach against medical pretrained LVLM methods (methods detailed in Section ) for VQA. Here too, JOMED delivered competitive performance relative to extensively pretrained models. For closed question tasks, JOMED with Pixtral and Qwen2-vl was superior to or matched current models. For open-ended question answering, JOMED with Qwen2-vl backbone matched LLaVA-Med<sub>Vicuna</sub> on the SLAKE dataset and achieved slightly lower results for PathVQA, showing a 0.01 - 0.02 token recall gap compared to pretrained LVLMs. Note that we do not compare our method on VQA-RAD, since our approach is trained on an internal split of training, validation, and test sets, whereas VQA-RAD provides only official training and test splits.

## Analysis

**JOMED boosts empirically challenging cases.** We observed that the performance gap is substantially larger for

Backbone	Model	Breast		Derma		Retina		VinDr		BRSET		VQA-RAD		SLAKE		Mean	Mean
		ACC	F1	ACC	F1	ACC	F1	ACC	F1	ACC	F1	Closed	Acc	Closed	Acc	ACC	F1
Qwen2-vl	Inconsistent	Reader	.40	.40	.50	.25	.35	.31	.41	.07	.33	.21	.43	.70	.40	.25	
		RAG	.40	.40	.52	.36	.40	.28	.46	.07	.49	.25	.33	.84	.45	.27	
		JOMED	<b>.80</b>	<b>.80</b>	<b>.62</b>	<b>.46</b>	<b>.52</b>	<b>.29</b>	<b>.48</b>	<b>.16</b>	<b>.50</b>	<b>.36</b>	<b>.47</b>	<b>.86</b>	<b>.58</b>	<b>.41</b>	
	Consistent	Reader	.84	.77	.83	.29	.63	.45	.56	.09	.34	.22	.77	.85	.64	.36	
		RAG	.86	.82	.90	.49	<b>.66</b>	.50	<b>.66</b>	<b>.10</b>	<b>.43</b>	.23	<b>.82</b>	.89	<b>.70</b>	.43	
		JOMED	<b>.88</b>	<b>.84</b>	<b>.91</b>	<b>.50</b>	<b>.66</b>	<b>.55</b>	<b>.66</b>	<b>.10</b>	.41	<b>.37</b>	<b>.82</b>	<b>.91</b>	<b>.70</b>	<b>.47</b>	
Pixtral	Inconsistent	Reader	.60	.59	.45	.33	.40	.32	.38	.07	.46	.28	.66	.64	.46	.32	
		RAG	.72	.71	.44	.45	.35	.37	.38	.08	.39	.26	.72	.65	.46	.37	
		JOMED	<b>.84</b>	<b>.84</b>	<b>.50</b>	<b>.50</b>	<b>.42</b>	<b>.46</b>	<b>.49</b>	<b>.13</b>	<b>.45</b>	<b>.35</b>	<b>.77</b>	<b>.68</b>	<b>.54</b>	<b>.46</b>	
	Consistent	Reader	.86	.80	.80	.56	.56	.44	.66	.08	.61	.37	.74	.85	.70	.45	
		RAG	<b>.91</b>	<b>.87</b>	.84	<b>.67</b>	<b>.62</b>	.50	<b>.71</b>	.08	<b>.64</b>	.38	<b>.75</b>	.91	.74	.50	
		JOMED	<b>.91</b>	<b>.87</b>	<b>.85</b>	<b>.67</b>	<b>.62</b>	<b>.53</b>	<b>.71</b>	<b>.10</b>	<b>.64</b>	<b>.42</b>	<b>.75</b>	<b>.91</b>	<b>.75</b>	<b>.52</b>	

Table 5: Analysis of joint training effect: for inconsistent retrieval predictions, we can see that applying joint training boosts performance significantly for all datasets. For consistent retrieval predictions, the results are slightly improved. Note that inconsistent retrievals are challenging to all models, even non-retrieval ones.

Model	Breast	Derma	Retina	VinDr	BRSET	VQARAD	SLAKE
Qwen2-vl	3%	51%	15%	50%	93%	12%	16%
Pixtral	16%	13%	16%	66%	70%	7%	8%

Table 6: Proportion of cases with inconsistent predictions, per dataset, for JOMED based on Qwen2-vl and Pixtral.

predictions classified as inconsistent retrieval predictions (the proportion of inconsistent retrieval predictions is reported in Table 6). We define an inconsistent retrieval prediction as one in which the model predicts different labels for retrieved candidates given the same target query (see Figure 1). Specifically, if the model’s predictions vary across retrieved candidates, the instance is categorized as an inconsistent retrieval prediction. Conversely, if the model consistently predicts the same label for all retrieved candidates, it is classified as a consistent retrieval prediction.

Both the consistent and inconsistent retrieval prediction sets are established after the initial reader training stage, and their performance is assessed following joint multimodal retriever fine-tuning. Detailed results are presented in Table 5. Overall, JOMED improves performance on inconsistent retrieval predictions by +0.12 in accuracy and +0.13 in F1 score when using the Qwen2-vl backbone, and by +0.09 in both accuracy and F1 score with the Pixtral backbone, while also offering a slight improvement on the consistent.

We also observed that inconsistent retrieval predictions are empirically more challenging for all models (both with and without retrieval). There is approximately a 10–20 point performance gap between the inconsistent and consistent.

**Performance with o3 as reranker.** We have observed that results for inconsistent predictions remain relatively low (Table 5), even after applying joint training (Table 5). However, in the oracle analysis reported above, we found that JOMED can sometimes retrieve images that lead to correct

predictions, together with other images that lead to wrong predictions. We thus explore whether a state-of-the-art multimodal model, when used as an optional reranker, could close the gap toward oracle performance for inconsistent retrieval predictions. Specifically, we investigated whether the o3 reasoning model (OpenAI 2025) could effectively select the image from the retrieved set that offers the most predictive information, guiding the model toward correct classification. We provided o3 with an image to classify, along with four retrieved images+captions, and tasked it with identifying the one containing the most predictive information. (detailed prompt in Appendix )

Our results show that o3’s performance generally surpasses simply taking the image with highest confidence, but o3 is generally inferior compared to fusing logits in JOMED. Thus, we were unable to bridge the gap to oracle performance, and conclude that reranking in this setting remains a significant challenge even for a frontier model. We report full results in Appendix .

**Additional analyses and ablations.** We include several robustness ablations and analyses in Appendix . We observed that our model is robust to scenarios where the retrieval is noisy or not given to the models. Further, we observed that the retrieval itself includes predictive knowledge without being given the query. details in Appendix .

## Conclusion

We explored the effectiveness of a multimodal retriever jointly optimized with a general-purpose LVLM. Our lightweight approach yielded substantial improvements, including in challenging cases involving inconsistent retrieval predictions. Our oracle analysis revealed a considerable performance gap between actual results and what was theoretically achievable using the retrieved images, providing a foundation for future research on closing this gap.

## References

- Agrawal, P.; Antoniak, S.; Hanna, E. B.; Bout, B.; Chaplot, D.; Chudnovsky, J.; Costa, D.; De Moncault, B.; Garg, S.; Gervet, T.; et al. 2024. Pixtral 12B. *arXiv preprint arXiv:2410.07073*.
- Al-Dhabyani, W.; Gomaa, M.; Khaled, H.; and Fahmy, A. 2020. Dataset of breast ultrasound images. *Data in brief*, 28: 104863.
- Casey, R. 2022.
- Chen, Z.; Wu, J.; Wang, W.; Su, W.; Chen, G.; Xing, S.; Zhong, M.; Zhang, Q.; Zhu, X.; Lu, L.; et al. 2024. Internvl: Scaling up vision foundation models and aligning for generic visual-linguistic tasks. In *Proceedings of the IEEE/CVF conference on computer vision and pattern recognition*, 24185–24198.
- He, S.; Nie, Y.; Chen, Z.; Cai, Z.; Wang, H.; Yang, S.; and Chen, H. 2024a. Meddr: Diagnosis-guided bootstrapping for large-scale medical vision-language learning. *CoRR*.
- He, S.; Nie, Y.; Wang, H.; Yang, S.; Wang, Y.; Cai, Z.; Chen, Z.; Xu, Y.; Luo, L.; Xiang, H.; et al. 2024b. Gsco: Towards generalizable ai in medicine via generalist-specialist collaboration. *arXiv preprint arXiv:2404.15127*.
- He, X.; Zhang, Y.; Mou, L.; Xing, E.; and Xie, P. 2020. Pathvqa: 30000+ questions for medical visual question answering. *arXiv preprint arXiv:2003.10286*.
- Hu, E. J.; Shen, Y.; Wallis, P.; Allen-Zhu, Z.; Li, Y.; Wang, S.; Wang, L.; and Chen, W. 2021. LoRA: Low-Rank Adaptation of Large Language Models. *arXiv:2106.09685*.
- Hu, Z.; Iscen, A.; Sun, C.; Wang, Z.; Chang, K.-W.; Sun, Y.; Schmid, C.; Ross, D. A.; and Fathi, A. 2023. Reveal: Retrieval-augmented visual-language pre-training with multi-source multimodal knowledge memory. In *Proceedings of the IEEE/CVF conference on computer vision and pattern recognition*, 23369–23379.
- Izacard, G.; Lewis, P.; Lomeli, M.; Hosseini, L.; Petroni, F.; Schick, T.; Dwivedi-Yu, J.; Joulin, A.; Riedel, S.; and Grave, E. 2023. Atlas: Few-shot learning with retrieval augmented language models. *Journal of Machine Learning Research*, 24(251): 1–43.
- Jeong, D. P.; Mani, P.; Garg, S.; Lipton, Z. C.; and Oberst, M. 2024. The Limited Impact of Medical Adaptation of Large Language and Vision-Language Models. *arXiv preprint arXiv:2411.08870*.
- Johnson, A. E.; Pollard, T. J.; Berkowitz, S. J.; Greenbaum, N. R.; Lungren, M. P.; Deng, C.-y.; Mark, R. G.; and Horng, S. 2019. MIMIC-CXR, a de-identified publicly available database of chest radiographs with free-text reports. *Scientific data*, 6(1): 317.
- Johnson, J.; Douze, M.; and Jégou, H. 2019. Billion-scale similarity search with GPUs. *IEEE Transactions on Big Data*, 7(3): 535–547.
- Lambert, B.; Forbes, F.; Tucholka, A.; Doyle, S.; Dehaene, H.; and Dojat, M. 2022. Trustworthy clinical AI solutions: a unified review of uncertainty quantification in deep learning models for medical image analysis. *arXiv preprint arXiv:2210.03736*.
- Lau, J. J.; Gayen, S.; Ben Abacha, A.; and Demner-Fushman, D. 2018. A dataset of clinically generated visual questions and answers about radiology images. *Scientific data*, 5(1): 1–10.
- Li, C.; Wong, C.; Zhang, S.; Usuyama, N.; Liu, H.; Yang, J.; Naumann, T.; Poon, H.; and Gao, J. 2023. Llava-med: Training a large language-and-vision assistant for biomedicine in one day. *Advances in Neural Information Processing Systems*, 36: 28541–28564.
- Lin, W.; Zhao, Z.; Zhang, X.; Wu, C.; Zhang, Y.; Wang, Y.; and Xie, W. 2023. Pmc-clip: Contrastive language-image pre-training using biomedical documents. In *International Conference on Medical Image Computing and Computer-Assisted Intervention*, 525–536. Springer.
- Lin, X. V.; Chen, X.; Chen, M.; Shi, W.; Lomeli, M.; James, R.; Rodriguez, P.; Kahn, J.; Szilvassy, G.; Lewis, M.; et al. 2024. Ra-dit: Retrieval-augmented dual instruction tuning. In *The Twelfth International Conference on Learning Representations*.
- Liu, B.; Zhan, L.-M.; Xu, L.; Ma, L.; Yang, Y.; and Wu, X.-M. 2021. Slake: A semantically-labeled knowledge-enhanced dataset for medical visual question answering. In *2021 IEEE 18th international symposium on biomedical imaging (ISBI)*, 1650–1654. IEEE.
- Liu, R.; Wang, X.; Wu, Q.; Dai, L.; Fang, X.; Yan, T.; Son, J.; Tang, S.; Li, J.; Gao, Z.; et al. 2022. Deepdrd: Diabetic retinopathy—grading and image quality estimation challenge. *Patterns*, 3(6).
- Luo, Y.; Zhang, J.; Fan, S.; Yang, K.; Wu, Y.; Qiao, M.; and Nie, Z. 2023. Biomedgpt: Open multimodal generative pre-trained transformer for biomedicine. *arXiv preprint arXiv:2308.09442*.
- Moor, M.; Huang, Q.; Wu, S.; Yasunaga, M.; Dalmia, Y.; Leskovec, J.; Zakka, C.; Reis, E. P.; and Rajpurkar, P. 2023. Med-flamingo: a multimodal medical few-shot learner. In *Machine Learning for Health (ML4H)*, 353–367. PMLR.
- Nakayama, L.; Goncalves, M.; Zago Ribeiro, L.; Santos, H.; Ferraz, D.; Malerbi, F.; et al. 2024. A brazilian multilabel ophthalmological dataset (BRSET). 2023. URL: <https://physionet.org/content/brazilian-ophthalmological/1.0.0/> [accessed 2024-08-14].
- OpenAI. 2025. OpenAI o3 and o4-mini System Card.
- Pham, H. H.; Tran, T. T.; and Nguyen, H. Q. 2022. VinDr-PCXR: An open, large-scale pediatric chest X-ray dataset for interpretation of common thoracic diseases. *PhysioNet (version 1.0.0)*, 10(2).
- Rückert, J.; Bloch, L.; Brüngel, R.; Idrissi-Yaghir, A.; Schäfer, H.; Schmidt, C. S.; Koitka, S.; Pelka, O.; Abacha, A. B.; G. Seco de Herrera, A.; et al. 2024. Rocov2: Radiology objects in context version 2, an updated multimodal image dataset. *Scientific Data*, 11(1): 688.
- Shi, W.; Min, S.; Yasunaga, M.; Seo, M.; James, R.; Lewis, M.; Zettlemoyer, L.; and Yih, W.-t. 2023. Replug: Retrieval-augmented black-box language models. *arXiv preprint arXiv:2301.12652*.

- Siriwardhana, S.; Weerasekera, R.; Wen, E.; Kaluarachchi, T.; Rana, R.; and Nanayakkara, S. 2023. Improving the domain adaptation of retrieval augmented generation (RAG) models for open domain question answering. *Transactions of the Association for Computational Linguistics*, 11: 1–17.
- Sun, J.; Zhang, J.; Zhou, Y.; Su, Z.; Qu, X.; and Cheng, Y. 2024. SURf: Teaching Large Vision-Language Models to Selectively Utilize Retrieved Information. In *EMNLP*.
- Thawakar, O. C.; Shaker, A. M.; Mullappilly, S. S.; Cholakkal, H.; Anwer, R. M.; Khan, S.; Laaksonen, J.; and Khan, F. 2024. XrayGPT: Chest radiographs summarization using large medical vision-language models. In *Proceedings of the 23rd workshop on biomedical natural language processing*, 440–448.
- Touvron, H.; Lavril, T.; Izacard, G.; Martinet, X.; Lachaux, M.-A.; Lacroix, T.; Rozière, B.; Goyal, N.; Hambro, E.; Azhar, F.; et al. 2023. Llama: Open and efficient foundation language models. *arXiv preprint arXiv:2302.13971*.
- Tschandl, P.; Rosendahl, C.; and Kittler, H. 2018. The HAM10000 dataset, a large collection of multi-source dermatoscopic images of common pigmented skin lesions. *Scientific data*, 5(1): 1–9.
- Wang, P.; Bai, S.; Tan, S.; Wang, S.; Fan, Z.; Bai, J.; Chen, K.; Liu, X.; Wang, J.; Ge, W.; et al. 2024. Qwen2-vl: Enhancing vision-language model’s perception of the world at any resolution. *arXiv preprint arXiv:2409.12191*.
- Wu, C.; Zhang, X.; Zhang, Y.; Wang, Y.; and Xie, W. 2023. Towards generalist foundation model for radiology by leveraging web-scale 2D&3D medical data. *arXiv preprint arXiv:2308.02463*.
- Wu, Y.; Lu, Y.; Zhou, Y.; Ding, Y.; Liu, J.; and Ruan, T. 2025. MKGF: A multi-modal knowledge graph based RAG framework to enhance LVLMs for Medical visual question answering. *Neurocomputing*, 129999.
- Xia, P.; Zhu, K.; Li, H.; Wang, T.; Shi, W.; Wang, S.; Zhang, L.; Zou, J.; and Yao, H. 2024a. Mmed-rag: Versatile multi-modal rag system for medical vision language models. *arXiv preprint arXiv:2410.13085*.
- Xia, P.; Zhu, K.; Li, H.; Zhu, H.; Li, Y.; Li, G.; Zhang, L.; and Yao, H. 2024b. Rule: Reliable multimodal rag for factuality in medical vision language models. In *Proceedings of the 2024 Conference on Empirical Methods in Natural Language Processing*, 1081–1093.
- Xiao, H.; Mastrapas, G.; and Wang, B. 2024. Jina CLIP: Your CLIP model is also your text retriever. In *Multi-modal Foundation Model meets Embodied AI Workshop@ICML2024*.
- Yang, J.; Shi, R.; Wei, D.; Liu, Z.; Zhao, L.; Ke, B.; Pfister, H.; and Ni, B. 2023. MedMNIST v2-A large-scale lightweight benchmark for 2D and 3D biomedical image classification. *Scientific Data*, 10(1): 41.
- Yoran, O.; Wolfson, T.; Ram, O.; and Berant, J. 2023. Making retrieval-augmented language models robust to irrelevant context. *arXiv preprint arXiv:2310.01558*.
- Yuan, Z.; Jin, Q.; Tan, C.; Zhao, Z.; Yuan, H.; Huang, F.; and Huang, S. 2023. Ramm: Retrieval-augmented biomedical visual question answering with multi-modal pre-training. In *Proceedings of the 31st ACM International Conference on Multimedia*, 547–556.
- Zhang, S.; Xu, Y.; Usuyama, N.; Xu, H.; Bagga, J.; Tinn, R.; Preston, S.; Rao, R.; Wei, M.; Valluri, N.; et al. 2023a. Biomedclip: a multimodal biomedical foundation model pretrained from fifteen million scientific image-text pairs. *arXiv preprint arXiv:2303.00915*.
- Zhang, X.; Wu, C.; Zhao, Z.; Lin, W.; Zhang, Y.; Wang, Y.; and Xie, W. 2023b. Pmc-vqa: Visual instruction tuning for medical visual question answering. *arXiv preprint arXiv:2305.10415*.
- Zheng, Y.; Zhang, R.; Zhang, J.; Ye, Y.; Luo, Z.; Feng, Z.; and Ma, Y. 2024. LlamaFactory: Unified Efficient Fine-Tuning of 100+ Language Models. In *Proceedings of the 62nd Annual Meeting of the Association for Computational Linguistics (Volume 3: System Demonstrations)*. Bangkok, Thailand: Association for Computational Linguistics.

## Dataset

### Dataset for Evaluation

Our datasets include real-world hospital datasets (BRSET (Nakayama et al. 2024) and VinDr-PCXR (Pham, Tran, and Nguyen 2022)) alongside a variety of classification and visual question answering datasets. We focus on a low-resource data-efficient setting (training sets ranging from 546 to 7007 samples in classification, 1790–19,700 in VQA). Medical image annotation is a resource-intensive task, demanding expert annotators whose availability is limited and expensive. Clinical AI also often has poor generalization across heterogeneous medical centers and patient populations, often requiring that models be trained for the specific context in which they are deployed (Casey 2022). Such constraints often restrict researchers to datasets comprising only a few thousand samples for a given study. Retrieval augmentation is well-suited for this setting, as it is known to benefit low-data regimes the most by leveraging external knowledge to compensate for sparse training samples. For the classification tasks, we used the following datasets:

BreastMNIST (nickname: Breast) (Al-Dhabyani et al. 2020) is a binary classification dataset of breast ultrasound. Following the official split, we use 546 for training, 78 for validation and 156 for testing.

RetinaMNIST (nickname: Retina) (Liu et al. 2022) is a multi-label classification dataset of retina Fundus Camera. Following the official split, we use 1,080 for training, 120 for validation and 400 for testing.

DermaMNIST (nickname: Derma) (Tschandl, Rosendahl, and Kittler 2018) is a multi-class classification dataset of common pigmented skin lesions. Following the official split, we use 7,007 for training, 1,003 for validation and 2,005 for testing. The dataset contains clinical images from 7 different diagnostic categories: actinic keratoses, basal cell carcinoma, benign keratosis, dermatofibroma, melanoma, melanocytic nevi, and vascular lesions.

VinDr-PCXR (Pham, Tran, and Nguyen 2022) is a large, open pediatric chest X-ray dataset collected in Vietnam

Backbone	Retrieval type	Breast		Derma		Retina		VQA-RAD		Mean	
		ACC	F1	ACC	F1	ACC	F1	ACC		ACC	F1
Flip a coin		.46	.30	.14	.10	.17	.16	.50	.35	.31	
Pixtral	WO Q img	.75	.42	.66	.18	.47	.33	.67	.67	.49	
	Reader only	.82	.66	.75	.53	.56	.44	.72	.74	.65	
	WO Retrieval	.84	.65	.78	.55	.58	.48	.72	.74	.65	
	Random Retrieval	.84	.69	.78	.56	.56	.45	.70	.74	.65	
Qwen2-vl	WO Q img	.81	.52	.56	.20	.47	.20	.70	.68	.48	
	Reader only	.82	.63	.68	.27	.61	.44	.74	.74	.59	
	WO Retrieval	.86	.70	.70	.33	.62	.42	.76	.76	.62	
	Random Retrieval	.85	.67	.73	.39	.63	.42	.77	.76	.62	

Table 7: We evaluate our models in three scenarios: (1) the model is not given the query image and must rely solely on the retrieved context for prediction; (2) the model is not given any retrieval; and (3) the model is given a retrieved context that is randomly chosen and may mislead it. We use two baselines: a random classifier (uniformly selects a class) and a reader-only model (trained without retrieval). We evaluate on Breast, Derma, Retina, and the closed-question subset of VQA-RAD.

(2020–2021) containing 9,125 posteroanterior scans from patients under 10 years old. It provides both lesion-level bounding-box annotations for 36 findings and image-level labels for multi-label of 15 diagnoses, curated by experienced radiologists. We follow the official split, which includes 7,728 training and 1,397 test images, with an additional internal split of the training data into 85% for training and 15% for validation.

BRSET (Nakayama et al. 2024) is a Brazilian multilabel ophthalmological dataset comprising retinal fundus images annotated with 14 distinct pathological findings. The dataset, composed of 16,266 images, presents a challenging real-world scenario for multilabel classification. There is no publicly available split; therefore, we apply an internal split for train, validation, and test sets (70% train, 10% validation, and 20% test).

Breast, Derma, and Retina taken from the large-scale MNIST-like collection of standardized biomedical images, including 12 datasets for 2D and 6 datasets for 3D. We especially used MedMNIST+ (Yang et al. 2023), which is a higher resolution extension of the original MedMNIST. We used the highest resolution of  $224 \times 224$ .

For medical question answering, we have three well-known datasets:

VQA-RAD (Lau et al. 2018) is a clinician-annotated visual question answering dataset focused on radiology images (e.g., X-ray, CT, MRI). It pairs each image with both open-ended and yes/no questions. Following the official split, we use 1,753 questions for training and 453 for testing. In addition, we further partition the training set into 85% for training and 15% for validation.

PathVQA (He et al. 2020) is a pathology-focused medical VQA dataset built from textbooks and the PEIR digital library, comprising 4,289 images and 32,632 question–answer pairs spanning both open-ended and yes/no questions. We follow the official split provided by the authors: 19,700 for training, 6,260 for validation, and 6,720 for testing.

SLAKE (Liu et al. 2021) is a bilingual medical VQA dataset. We use the English subset, *SLAKE-English*, which

comprises 642 radiology images and 7.03k English QA pairs. We follow the official train/validation/test split of 4.92k/1.05k/1.06k QA pairs, and include all question types, covering both open-ended and closed-ended formats.

## Dataset for Index

For construction of the Index we used three large datasets of (image, text) pairs: PMC-OA (Lin et al. 2023), ROCO (Rückert et al. 2024) and MIMIC-CXR (Johnson et al. 2019):

PMC-OA: is a large-scale dataset that contains 1.65M image-text pairs. The figures and captions from PubMed Central, 2,478,267 available papers are covered.

ROCO: is an image-caption dataset collected from PubMed. It filters out all the compound or non-radiological images, and consists of 81K samples.

MIMIC-CXR: is the largest chest X-ray dataset, containing 377,110 samples (image-report pairs). Each image is paired with a clinical report describing findings from doctors.

## Implementation Details

### Retrieval Augmentation

As described earlier, for each image–question pair, we retrieve  $r$  image–text pairs, with  $r = 4$ . We use the input image as the query and Jina-CLIP (Xiao, Mastrapas, and Wang 2024) as the retriever head in our multimodal retriever. The index is constructed with FAISS (Johnson, Douze, and Jégou 2019) over MIMIC-CXR, PMC-OA, and ROCO, which are fully described in Section in Appendix A. To embed images, we use the Jina-CLIP visual head (the same model used for retrieval); to embed captions/reports, we use the Jina-CLIP text head. The index is stored in `float16` due to storage constraints. We also experimented with Biomed-CLIP (Zhang et al. 2023a).

Backbone	Model	Breast		Derma		Retina	
		ACC	F1	ACC	F1	ACC	F1
Qwen2-vl	Top-1	.50	.60	.32	.25	.38	.32
	Top-1 logits	.60	.58	.43	.35	.37	.38
	o3	.77	.80	.42	.32	.35	.33
	o3 multi-image	.77	.80	.43	.33	.43	.35
	JOMED	.77	.80	.57	.43	.51	.47
Pixtral	Top-1	.72	.75	.46	.48	.29	.33
	Top-1 logits	.64	.63	.40	.40	.29	.32
	o3	.73	.73	.42	.37	.25	.30
	o3 multi-image	.73	.73	.43	.42	.34	.37
	JOMED	.76	.77	.45	.47	.34	.37

Table 8: Study of o3 as a reranker. We evaluate o3’s ability to rerank the inconsistent predictions, selecting which of the retrieved (image, caption) pairs has the most predictive information for the query image. We compared the performance of choosing the highest similarity retrieved (image, caption) pair, choosing the highest confidence (top logits), using only the caption for reranking, and using our current strategy of fusing logits from all predictions. The metrics used are accuracy and F1 score.

## Reader Fine-Tuning

We use Pixtral (12B) (Agrawal et al. 2024) and Qwen2-vl (7B) (Wang et al. 2024) as base models. We train the models with and without retrieval augmentation to assess their effect. The retrieval-augmented prompt is described in Appendix E. Note, we also tried Med-Flamingo (9B) (Moor et al. 2023) as a base model.

We fine-tune Pixtral and Qwen2-vl using LLaMA-Factory (Zheng et al. 2024) on a single NVIDIA L40 (48 GB) GPU for 10 epochs. We use a learning rate of  $2 \times 10^{-5}$  and apply Low-Rank Adaptation (LoRA) (Hu et al. 2021) for parameter-efficient fine-tuning. To all models (including baseline models), we conduct a grid search over batch size (2, 4, 6) and whether to freeze the vision head, selecting the best configuration by validation performance. For Med-Flamingo, we fine-tune using our codebase on a single NVIDIA L40 (48 GB) GPU for 10 epochs. Following the Med-Flamingo paper, the language model and image encoder are frozen, and only the Gated Cross-Attention layers and the Perceiver Resampler are optimized for stable and efficient learning. We use a learning rate of  $2 \times 10^{-5}$ .

## Multimodal Retriever Fine-Tuning

We train the retrieval model to fetch relevant context while keeping the reader frozen. We use Jina-CLIP’s visual head as the base model for the multimodal retriever. The model is trained on a single NVIDIA L40 (48 GB) GPU for 100 epochs with a learning rate of  $2 \times 10^{-5}$ , freezing all layers except the last ten. We set the number of retrieved candidates per query to 50. In our experiments, retrieving more candidates further improved retriever performance.

## Evaluation Metrics

**Classification.** We report Accuracy (ACC) and Macro F1:

$$\text{ACC} = \frac{1}{N} \sum_{n=1}^N \mathbf{1}[\hat{y}_n = y_n],$$

$$\text{MacroF1} = \frac{1}{C} \sum_{c=1}^C \frac{2 \text{Prec}_c \text{Rec}_c}{\text{Prec}_c + \text{Rec}_c},$$

where  $\text{Prec}_c$  and  $\text{Rec}_c$  are precision and recall computed per class  $c$ ,  $C$  is the number of classes, and  $N$  is the number of examples.

**Visual Question Answering (VQA).** For open-ended questions, we compute token-level Recall and F1 between the predicted token set  $\hat{A}$  and the reference token set  $A$ :

$$\text{Prec} = \frac{|\hat{A} \cap A|}{|\hat{A}|}, \quad \text{Rec} = \frac{|\hat{A} \cap A|}{|A|}, \quad \text{F1} = \frac{2 \text{Prec} \cdot \text{Rec}}{\text{Prec} + \text{Rec}}.$$

For closed-ended questions, we use Exact Match.

## Baseline Methods

We benchmark against state-of-the-art medical large vision-language models (LVLMs) that underwent large-scale medical pre-training:

**BiomedGPT.** An open multimodal generative pre-trained transformer for biomedicine that aligns diverse biological/biomedical modalities with natural language; we include it as a strong domain baseline (Luo et al. 2023).

**LLaVA-Med.** A biomedical adaptation of LLaVA trained via curriculum (biomedical figure–caption alignment followed by instruction tuning); we evaluate three commonly used releases as separate baselines (Li et al. 2023).

**MedViNT-TE and MedViNT-TD.** Two implementations of Medical Visual Instruction Tuning from PMC-VQA (Zhang et al. 2023b). Both adopt a PMC-CLIP vision encoder (Lin et al. 2023). TE uses an encoder-style text pathway feeding a multimodal decoder, while TD concatenates text tokens with visual features to a decoder-only pathway; we report both as distinct baselines.

**InternVL-based baselines: MedDr, MedDr+RAD, and GSCo.** **MedDr** is a generalist medical VLLM trained on large-scale instruction-style data curated from diagnosis-guided bootstrapping and medical image descriptions, covering multiple modalities and tasks (He et al. 2024a).

**MedDr+RAD** augments MedDr at inference with Retrieval-Augmented Diagnosis (RAD): for a test image, similar cases are retrieved and summarized as contextual guidance in the prompt (He et al. 2024b). **GSCo** (Generalist-Specialist Collaboration) is a two-stage framework that (i) builds a generalist GFM (MedDr) and lightweight specialist models, and (ii) performs collaborative inference via Mixture-of-Expert Diagnosis (MoED; using specialist predictions as references) and RAD (using specialists to retrieve similar cases) (He et al. 2024b). GSCo evaluates across a large multi-dataset benchmark; we include GSCo

Backbone	BiomedCLIP Variant	Breast		Derma		Retina		Vindr		BREST		VQA-RAD		SLAKE		PathVQA		Mean	
		ACC	F1	ACC	ACC	ACC	ACC	ACC	ACC	ACC	F1								
Qwen2-vl	FT RAG	.84	.81	.73	.38	.63	.45	.54	.09	.49	.27	.77	.89	.92	.72	.40			
	JOMED	<b>.87</b>	<b>.82</b>	<b>.75</b>	<b>.40</b>	<b>.65</b>	<b>.50</b>	<b>.58</b>	<b>.15</b>	<b>.50</b>	<b>.39</b>	<b>.79</b>	<b>.91</b>	<b>.92</b>	<b>.74</b>	<b>.45</b>			
Pixtral	FT RAG	.88	.84	.79	.57	.57	.46	.55	.09	.44	.31	.74	.87	.88	.72	.45			
	JOMED	<b>.91</b>	<b>.87</b>	<b>.80</b>	<b>.59</b>	<b>.59</b>	<b>.49</b>	<b>.56</b>	<b>.15</b>	<b>.50</b>	<b>.39</b>	<b>.77</b>	<b>.89</b>	<b>.89</b>	<b>.74</b>	<b>.50</b>			

Table 9: Performance comparison of JOMED against FT RAG baseline across medical imaging classification and VQA tasks. Both Qwen2-VL and Pixtral backbones show consistent improvements with JOMED, particularly in F1 scores. Results demonstrate that BiomedCLIP-based retrieval enhances performance similarly to the general-purpose retriever. VQA results are reported for the closed-question subset using exact match accuracy.

MedFlamingo Variant	Breast		Derma		Retina		VQARAD		ACC
	ACC	F1	ACC	F1	ACC	F1	ACC	ACC	
Reader only	<b>.82</b>	<b>.77</b>	.67	<b>.54</b>	.57	.40		.65	
JOMED	.81	<b>.77</b>	<b>.68</b>	<b>.54</b>	<b>.60</b>	<b>.51</b>		<b>.69</b>	

Table 10: Med-Flamingo comparison with and without JOMED retrieval augmentation across medical imaging tasks. JOMED achieves best performance on 4 out of 7 metrics, with notable improvements over Reader Only in Retina classification (ACC: 0.57→0.60, F1: 0.40→0.51) and VQA-RAD (0.65→0.69). However, the overall performance gains are more modest than those observed with other backbone architectures, indicating that Med-Flamingo may have limited capacity to leverage additional retrieval context.

as a strong InternVL-based baseline along with its MedDr and MedDr+RAD components (He et al. 2024b; Chen et al. 2024).

## Additional Analysis

### Performance with a State-of-the-Art LVLM Reranker

We evaluate whether a state-of-the-art large vision–language model (LVLM), used as an optional reranker, can improve performance on inconsistent-retrieval predictions. Specifically, we test the o3 reasoning model (OpenAI 2025) as a reranker: given a query image to classify and four retrieved image–caption pairs, o3 is asked to select the single pair that is most informative for predicting the correct label. We compare this reranking to four alternatives: (i) using the top-1 retrieved candidate (no reranking), (ii) selecting the model’s prediction with the highest confidence (maximum logit), (iii) using o3 with captions only (no images), and (iv) the JOMED aggregation strategy.

Our results show that o3 generally outperforms the maximum-logit baseline but remains inferior to JOMED’s logit-fusion aggregation. We evaluated performance on the Breast, Derma, and Retina datasets. For the remaining datasets—VinDr-PCXR, BRSET, and the visual question

answering (VQA) datasets—we did not run this evaluation because the images and/or retrieved candidates come from restricted-access sources (e.g., MIMIC-CXR, VinDr-PCXR, and BRSET). See results in Table 8.

### JOMED variants with medical pre-trained backbones

Although our work focuses on general-purpose LVLMs, we also evaluated a medical-specific baseline. We conducted the evaluation on four benchmarks—Breast, Derma, Retina, and VQA-RAD (closed-question subset). For the medical pre-trained baseline, we used Med-Flamingo and paired it with a medically pre-trained retriever (BiomedCLIP), using only one retrieval head (image retrieval without text retrieval). The performance gap between Med-Flamingo and our reader approach was small—0.01 in accuracy and 0.03 in F1. We hypothesize that this narrow gap may be due to Med-Flamingo’s relatively older LLaMA backbone (Touvron et al. 2023). Results are presented in Table 10. We also tested our general-purpose backbone with a medically pre-trained retriever, which showed improvements over FT RAG, with a similar pattern to the general-purpose retriever. Full results are presented in Table 9.

### Retrieval Robustness Analyses.

We strive for our model to be robust in cases where the retrieval is noisy. Meaning, that the intrinsic ability in the model parameters is not overly dependent on the retrieval content. To test this property without ground truth retrieval labels, we evaluate the model performance with random candidates instead of searching according to cosine similarity. Overall as shown in Table 7 in Appendix D, we observed that for all datasets the model performance is above the reader-only, showing the model succeeded more than a model trained without any retrieval.

We also test the ability of the model to still function without any retrieved context. We do this to check whether some intrinsic capability is still maintained in the model’s reader without any retrieved information. This could also be helpful in cases where model users would like it to be versatile and support both retrieval-augmented prediction and non-retrieval-augmented prediction (e.g., in cases where no retrieved contexts were discovered). As shown in Table 7 in

Appendix D, removing retrieval from JOMED resulted in performance comparable or slightly lower than the reader-only model.

Finally, we tested the model without the input image, relying only on the (image, report / caption) retrievals, to further assess the information held in retrieved data for predictions. In this scenario, we expected a substantial performance drop because the model no longer had direct knowledge of the patient’s condition, aside from what was provided by retrieved candidates. As a baseline, we used a simple random guess (coin flip), representing a scenario in which retrieval was not used effectively. As shown in Table 7 in Appendix D, our model’s performance exceeded this baseline by a large margin, with improvements of 0.32 in Accuracy, 0.28 in F1. These results indicate that the model learns from the retrieved data, yet it does not become overly dependent on it as we previously showed.

### **Prompt Design**

Here, we detail the prompts used in our experiments and analysis. To explore the utility of o3 as re-rankers of the most predictive (image, caption) pair, as described in Section in Appendix D, we provide both models with a detailed prompt for the task, shown in Prompt 1.

Additionally, we present the prompts used to train JOMED for each of the datasets: Prompts 2, 4, 3, 6, 5, and the prompt for visual question answering tasks Prompt 7.

```

1 Task:
2
3 You are an expert assistant selecting the most informative reference for medical image
4 classification.
5
6 Description:
7 A patient's [MRI/CT/X-ray] image needs to be classified into one of the following
8 categories: [List of possible labels].
9 You are given four candidate reference pairs, each consisting of a caption and its
10 associated image, drawn from PubMed literature.
11 Your goal is to determine which single candidate provides the most useful information
12 to help an AI model correctly classify the provided image.
13
14 Input Information:
15 - Medical image: The patient's MRI/CT/X-ray image is provided here.
16 - Classification task: Classify the image into one of the following categories: [List
17 of possible labels].
18 - Candidates:
19     - Candidate 0:
20         - Caption: [Caption 0]
21         - Image: [Image 0]
22     - Candidate 1:
23         - Caption: [Caption 1]
24         - Image: [Image 1]
25     - Candidate 2:
26         - Caption: [Caption 2]
27         - Image: [Image 2]
28     - Candidate 3:
29         - Caption: [Caption 3]
30         - Image: [Image 3]
31
32 Instructions:
33 1. For each candidate, carefully assess how informative its caption and image are for
34 the current classification task.
35 2. Specifically, evaluate whether the candidate describes imaging features, findings,
36 or clinical context relevant to distinguishing among the listed categories.
37 3. Compare all candidates and select the one that gives the clearest, most
38 discriminative information to aid the classification.
39 4. Output only the number of the selected candidate in the following format:
40     Caption Number: [your selected number]

```

Listing 1: Prompt used for o3

```

1 <retrieved image>background:<
2 retrieved text>\n\n<query image>Does
3 this breast ultrasound image show
4 signs of cancer?

```

Listing 2: Prompt used by JOMED for Breast classification

```

1 <retrieved image>background:<
2 retrieved text>\n<query image>what is
3 the severity of diabetic retinopathy?

```

Listing 3: Prompt used by JOMED for Retina classification

```

1 <retrieved image>background:<retrieved text>\n\nProvide answer according to the
2 labels:\n"
3 "0 - 'Actinic keratoses and intraepithelial carcinoma'\n"
4 "1 - 'Basal cell carcinoma'\n"
5 "2 - 'Benign keratosis-like lesions'\n"
6 "3 - 'Dermatofibroma'\n"
7 "4 - 'Melanoma'\n"
8 "5 - 'Melanocytic nevi'\n"
9 "6 - 'Vascular lesions'\n\n<query image>What type of skin lesion does the
10 patient have?

```

Listing 4: Prompt used by JOMED for Derma classification

```

1 <retrieved image>background:<retrieved text> Provide answer according to the labels
2 :\n
3 0 - 'No finding'\n
4 1 - 'Bronchitis'\n
5 2 - 'Brocho-pneumonia'\n
6 3 - 'Other disease'\n
7 4 - 'Bronchiolitis'\n
8 5 - 'Situs inversus'\n
9 6 - 'Pneumonia'\n
10 7 - 'Pleuro-pneumonia'\n
11 8 - 'Diaphragmatic hernia'\n
12 9 - 'Tuberculosis'\n
13 10 - 'Congenital emphysema'\n
14 11 - 'CPAM'\n
15 12 - 'Hyaline membrane disease'\n
16 13 - 'Mediastinal tumor'\n
17 14 - 'Lung tumor'\n\n
18 \n\n<image>Question: Look at this X-ray scan and select all abnormalities you see
from the given labels Answer:

```

Listing 5: Prompt used by JOMED for Vindr-PCXR classification

```

1 <retrieved image>background:<retrieved text> Provide answer according to the labels:\n
2 0 - 'no findings'\n
3 1 - 'diabetic_retinopathy'\n
4 2 - 'macular_edema'\n
5 3 - 'scar'\n
6 4 - 'nevus'\n
7 5 - 'amd'\n
8 6 - 'vascular_occlusion'\n
9 7 - 'hypertensive_retinopathy'\n
10 8 - 'drusens'\n
11 9 - 'hemorrhage'\n
12 10 - 'retinal_detachment'\n
13 11 - 'myopic_fundus'\n
14 12 - 'increased_cup_disc'\n
15 13 - 'other'\n\n
16 \n\n<image>Question: Look at retinal fundus image and select all abnormalities you see
from the given labels

```

Listing 6: Prompt used by JOMED for BRSET classification

```
1      <retrieved image>background:<
  retrieved text>\n<query image><query
  question>?
```

Listing 7: Prompt used by JOMED for visual question answering tasks